Indoor Atmospheric Nanocluster Aerosol Dynamics in Residential Buildings

Satya S. PATRA[1], Gerhard STEINER[2], Nusrat JUNG[1], Brandon E. BOOR[1]*

[1]Purdue University, Lyles School of Civil Engineering,
West Lafayette, Indiana, USA

[2]GRIMM Aerosol Technik Ainring GmbH & Co. KG,
Ainring, Germany

* Corresponding Author (email: bboor@purdue.edu)

ABSTRACT

Sub-3 nm nanocluster aerosol (NCA) represent a critically important, yet understudied, class of atmospheric aerosol particles. The behavior and prevalence of indoor atmospheric NCA are likely to be influenced by a variety of building and occupant characteristics. Given the nature of human activities in indoor spaces, NCA sources are likely to be highly transient, resulting in rapidly changing indoor NCA concentrations over short timescales. However, a complete mechanistic understanding of the formation, transformation, and exposure of indoor atmospheric NCA down to 1 nm in residential buildings is presently lacking. Field measurements of the formation and growth of indoor atmospheric NCA during common household activities were conducted in a mechanically ventilated residential building – the Purdue zero Energy Design Guidance for Engineers (zEDGE) Tiny House. Particle number size distributions from 1.18 to 30,000 nm were measured using a suite of aerosol instrumentation, including a particle size magnifier – scanning mobility particle sizer (PSMPS), a SMPS with a long differential mobility analyzer (DMA), and a wideband integrated bioaerosol sensor (WIBS). Additionally, a comprehensive material balance model was developed, integrating complex physical transformation processes such as nucleation, intermodal and intramodal coagulation, condensation, deposition, and ventilation, to understand the transformation of indoor atmospheric NCA.

The results reveal unique dynamics and heightened inhalation exposure to indoor atmospheric NCA during common household activities. First, during indoor combustion activities such as cooking, NCA persisted throughout the active combustion period despite their tendency to coagulate and diffuse to surfaces. Second, the primary mechanisms driving the loss of indoor atmospheric NCA are coagulation, followed by condensation, deposition, and ventilation. Interestingly, the presence of larger particles was observed to suppress the persistence of indoor atmospheric NCA through coagulation scavenging. Furthermore, indoor atmospheric NCA could not be adequately modeled using conventional indoor air pollution markers, such as fine particulate matter ($PM_{2.5}$) mass concentrations and NO_x ($NO+NO_2$) mixing ratios. Considering that people spend approximately 90% of their time indoors, understanding the unique behaviors and transformations of indoor atmospheric NCA is critical for assessing and mitigating potential human health risks associated with indoor air pollution in residential buildings.

1. INTRODUCTION

Atmospheric nanocluster aerosol (NCA) – tiny molecular clusters with diameters ranging from 1 to 3 nanometers – constitute the largest portion of nucleation mode particles from primary and secondary nanoparticle emission sources (Kontkanen et al., 2017; Patra et al., 2024; Rosales et al., 2022). While research on emissions of larger atmospheric particles has been thoroughly explored indoors (Audignon-Durand et al., 2023), there is limited information available on indoor atmospheric NCA emissions due to the analytical challenges in measuring them (Kangasluoma et al., 2020). However, the difficulty in measuring NCA does not mean they can be overlooked. NCA have several orders of magnitude higher surface area-to-volume ratios than other sub-100 nm particles, indicating a potentially higher risk of bioactivity and toxicity. When inhaled, NCA are deposited in the upper respiratory tract and the tracheobronchial region at a significantly higher rate than other sub-100 nm particles (Patra et al., 2024). Once deposited, they can move between cells, infiltrate into the bloodstream, and potentially translocate to vital organs such as the liver and brain (Peters et al., 2011). Studies have shown that NCA can induce cytotoxic, apoptotic, and proinflammatory effects in eukaryotic and endothelial cells (Sgro et al., 2009). Given these reasons, it is necessary to investigate indoor

atmospheric NCA emissions, their transformations, and inhalation exposures during common household activities that either directly emit NCA or form NCA through oxidation processes.

Indoor atmospheric NCA dynamics are inherently influenced by multifaceted factors, including the emission source, aerosol physics, and building-related factors, such as ventilation conditions and the abundance of surfaces available for deposition. However, a complete mechanistic model that incorporates all these factors to study indoor atmospheric NCA emissions and transformations down to 1 nm is currently lacking. Considering the aspects of human activities occurring indoors, it is expected that NCA dynamics are exceedingly transient, causing concentrations to change rapidly over short periods. Here, we develop a generalizable model for indoor atmospheric NCA dynamics inspired by the aerosol general dynamics equation and incorporating building-related factors to accurately model size-resolved NCA emission and nucleation rates. We utilized this model with real-world, high-resolution NCA measurements in a full-scale, single-zone test house during common household activities, such as cooking, burning scented candles, and cleaning, to provide new insights into indoor atmospheric NCA dynamics in residential buildings. Furthermore, our model can be extended to explore how advanced HVAC control systems and filter-based air purifier technologies in high performance buildings affect the rate of change in indoor atmospheric NCA concentrations during such activities. This could help manage occupants' exposure to indoor atmospheric NCA, enhancing indoor air quality and occupants' health and safety in residential and office environments.

2. METHODS

2.1 Field Measurement Campaign and Instrumentation

We conducted a field measurement campaign to assess indoor atmospheric NCA dynamics in a single-zone, mechanically ventilated residential building – the Purdue zero Energy Design Guidance for Engineers (zEDGE) test house (Jiang et al., 2023). zEDGE is situated on the Purdue University campus in West Lafayette, Indiana, USA. It is built on a mobile trailer following the standards set by the recreational vehicle industry association (RVIA) and holds a certification from the national organization of alternative housing (NOAH). The interior of zEDGE is air-conditioned, spans 60.35 m^3, and is split into the main floor and a loft space. The house features a single-zone ductless heating and cooling system and a portable air conditioning unit. A variable-speed powered ventilator, equipped with two MERV 13 filters, was used to bring filtered outdoor air into the test house. To establish variable outdoor air ventilation rates, we adjusted the settings of the air conditioning unit and the powered ventilator. Four fans were installed in the main and loft areas of zEDGE to ensure uniform mixing of indoor air. We assessed this mixing state using four portable diffusion chargers, measuring particles between 10 to 2,500 nm, and concluded that the air inside was well-mixed, attributed to the use of these fans.

Indoor particle number concentrations and size distributions, ranging from 1.18 to 30,000 nm, were measured using an array of online aerosol instrumentation. This included a novel particle size magnifier – scanning mobility particle sizer (PSMPS), a scanning mobility particle sizer (SMPS) with a long differential mobility analyzer (DMA), and a wideband integrated bioaerosol sensor (WIBS). The PSMPS is a new two-stage mobility particle size spectrometer for electrical mobility-classified measurements of atmospheric NCA. It is configured with a soft X-ray neutralizer, a Vienna-type modified short-DMA, a diethylene glycol-based particle size magnifier (PSM), and a butanol-based condensation particle counter (CPC). The SMPS includes a Kr-85 bipolar charger, a long-DMA, and a water-based CPC. Lastly, the WIBS features a 635 nm continuous laser diode to detect and size particles. The PSMPS measured particles from 1.18 to 55.7 nm, the SMPS measured particles from 13.1 to 572.5 nm, and the WIBS measured particles from 500 to 30,000 nm. The data from all three instruments were merged using a moving average smoothing method. A detailed description of the instrument setup and aerosol data analysis is available elsewhere (Patra et al., 2024). The layout of the aerosol instrumentation in the Purdue zEDGE test house during the field measurement campaign is shown in Fig. 1. Additional air quality instruments utilized in this study included a NO_x (NO and NO_2) analyzer, an ozone (O_3) analyzer, a carbon dioxide (CO_2) analyzer, and a handheld humidity and temperature meter. Indoor atmospheric volatile organic compound (VOC) mixing ratios were measured in real-time using a proton transfer reaction time-of-flight mass spectrometer (PTR-TOF-MS) (Jiang et al., 2023; Liu et al., 2024).

During the field measurement campaign, a number of controlled, simulated experiments replicating common household activities were conducted in the zEDGE test house. This study discusses a subset of the events, which include boiling water, cooking buttermilk pancakes and grilled cheese sandwiches, burning scented candles, and indoor mopping. The experiments began at time zero, with two experimenters entering the Purdue zEDGE test house.

For the initial 10 minutes, no activities were performed in the test house, establishing a baseline concentration of indoor air pollutants with people present. At the 10-minute mark, the source activity (e.g., boiling water, cooking, etc.) was initiated and continued for the next 20 minutes (10 minutes for the indoor mopping activities). Upon reaching the 30-minute mark (20-minute mark for the indoor mopping activities), the activities were concluded, and the experimenters exited the test house. Finally, the decay in the emitted air pollutants was observed in the unoccupied test house.

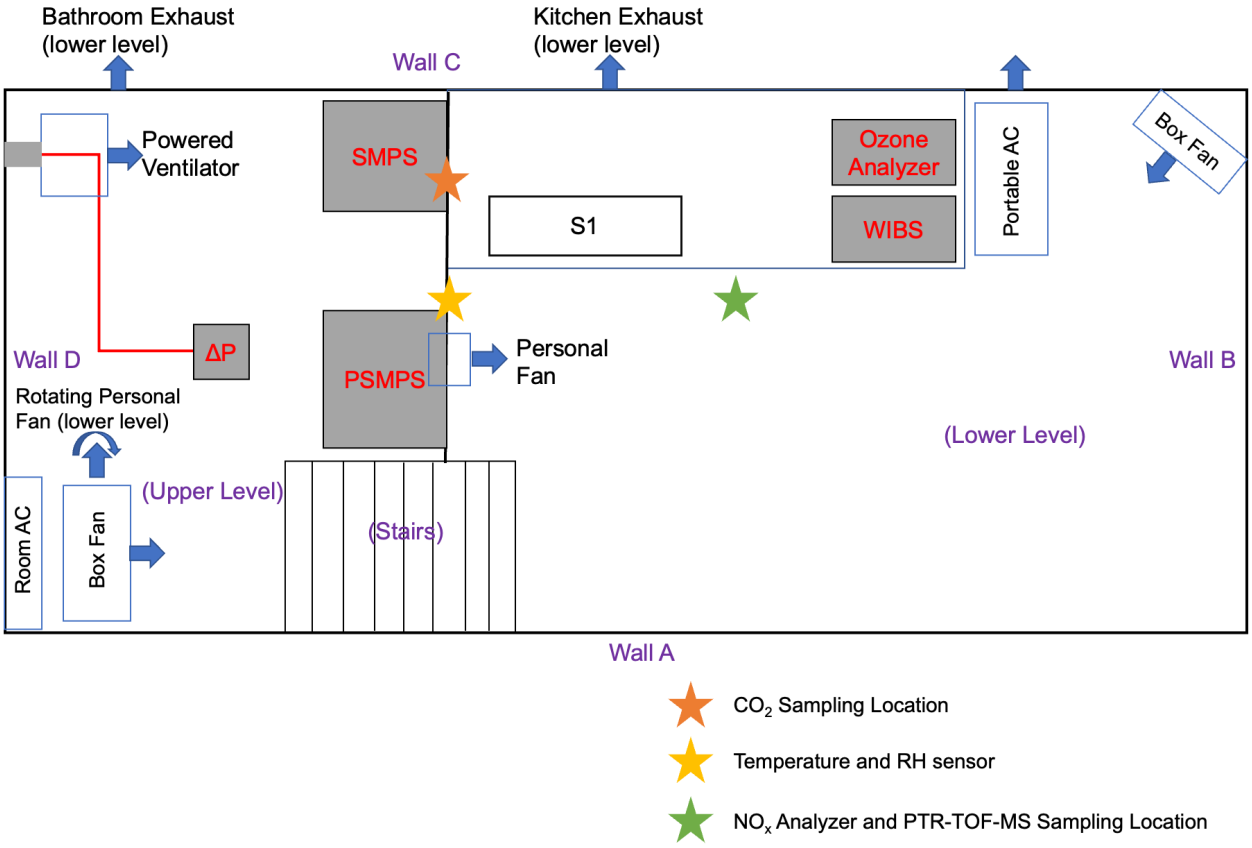

Figure 1: Experimental layout of the Purdue zEDGE test house and aerosol instrumentation for the field measurement campaign. S1 is the location where the gas stove and candles were placed for the experiments. For the mopping experiments, the lower level floor was mopped.

2.1 Modeling Indoor Atmospheric NCA Dynamics in Residential Buildings

We have developed a generalized indoor atmospheric NCA general dynamics model inspired by the aerosol general dynamics equation (Kulmala et al., 2012). Our model, which fundamentally relies on the principle of mass conservation, uses equations derived from tracking the formation and removal of NCA in a Eulerian domain to mechanistically connect outcome variables with key input parameters. The key physical transformation processes include emission/nucleation, intermodal and extramodal coagulation, condensation, surface deposition, ventilation (pathways include mechanical, natural, and infiltration), and removal via filter-based air purifiers. This offers a comprehensive framework to examine the fate of indoor atmospheric NCA, expressed as shown in equation (1).

$$\frac{dN_{d_{p,i}}}{dt} = E_{d_{p,i,app}} + \left(k_{vent,m}\left(1-\eta_{d_{p,i}}\right) + k_{vent,n} + k_{vent,l}\cdot P_{d_{p,i}}\right)\cdot N_{out,d_{p,i}} - k_{ap,d_{p,i}}\cdot N_{d_{p,i}} - \left(k_{vent,m} + k_{vent,n} + k_{vent,l}\right)\cdot N_{d_{p,i}} - k_{dep,d_{p,i}}\cdot N_{d_{p,i}} - CoagSnk_{d_{p,i}}\cdot N_{d_{p,i}} + CoagSrc_{d_{p,i}} - Cond_{d_{p,i}} + Cond_{(d_{p,i-1})} \quad (1)$$

In equation (1), $N_{d_{p,i}}$ and $N_{out,d_{p,i}}$ are the indoor and outdoor particle number concentrations [cm^{-3}], respectively, in size bin i as characterized by the midpoint diameter, d_p, in the PSMPS. $\frac{dN_{d_{p,i}}}{dt}$ is the time derivative of $N_{d_{p,i}}$ [cm^{-3} min^{-1}]. $E_{d_{p,i,app}}$ is the size-dependent apparent emission rate of particles at size d_p [cm^{-3} min^{-1}]. $k_{vent,m}$ [min^{-1}], $k_{vent,n}$ [min^{-1}], and $k_{vent,l}$ [min^{-1}] are the nominal outdoor air ventilation rates through mechanical ventilation, natural ventilation, and infiltration through leakage across the building envelope, respectively. $\eta_{d_{p,i}}$ is the size-dependent single-pass removal efficiency of the filter used in the mechanical ventilation system. $P_{d_{p,i}}$ is the size-dependent penetration efficiency of particles across the leakage flow path. $k_{ap,d_{p,i}}$ is the size-dependent first-order removal rate coefficient of particles at size d_p through a filter-based air purifier [min^{-1}]. $k_{dep,d_{p,i}}$ is the size-dependent first-order deposition loss rate coefficient of particles at size d_p [min^{-1}]. $CoagSnk_{d_{p,i}}$ is the coagulation sink of particles at size d_p [min^{-1}]; and $CoagSrc_{d_{p,i}}$ is the coagulation source of particles at size d_p [cm^{-3} min^{-1}]. $Cond_{d_{p,i}}$and $Cond_{(d_{p,i-1})}$ are the net condensational loss and source of particles at size d_p due to the condensation of low volatility vapors [cm^{-3} min^{-1}].

In our field measurement campaign, the Purdue zEDGE test house featured only mechanical ventilation and no air purifiers were used indoors. We also assumed negligible outdoor-to-indoor NCA transport through the mechanical ventilation system and negligible NCA infiltration through the building envelope. This simplified equation (1) to the expression shown in equation (2).

$$\frac{dN_{d_{p,i}}}{dt} = E_{d_{p,i,app}} - k_{vent,m} \cdot N_{d_{p,i}} - k_{dep,d_{p,i}} \cdot N_{d_{p,i}} - CoagSnk_{d_{p,i}} \cdot N_{d_{p,i}} + CoagSrc_{d_{p,i}} - Cond_{d_{p,i}} + Cond_{(d_{p,i-1})} \quad (2)$$

Equation (2) can be rearranged and integrated over the NCA size fraction to obtain the apparent size-integrated NCA emission rate ($E_{NCA,app}$; cm^{-3} min^{-1}). The mathematical formulation of coagulation sinks and sources, as well as condensation sinks and sources, can be found in Patra et al., 2024. The net difference between the coagulation sink and the source, termed as the net coagulation sink ($CoagSnk_{Net}$; s^{-1}), effectively captures the net effect of coagulation scavenging on particles of size d_p (Patra et al., 2024). Equation (1), with minor modifications, can also be applied to calculate the nucleation rate of particles (Cai & Jiang, 2017). We also modeled the condensational growth of NCA into larger particles, denoted as GR_{Cond} [nm h^{-1}]. GR_{Cond} is determined using the mode-fitting method and is adjusted for the growth rate attributable to both intramodal and intermodal coagulation (Stolzenburg et al., 2023). Furthermore, based on the methods outlined in previously published studies (Jiang et al., 2021; Patra et al., 2024), we estimated the size-integrated NCA respiratory tract deposited dose rates ($R_{D,NCA}$; min^{-1}) for adults. These estimates used measured NCA number concentrations during the household activities and the size-resolved deposition fraction of particles in each region of the human respiratory tract (head airways, tracheobronchial, and pulmonary) to evaluate human exposure to NCA during these activities.

3. RESULTS AND DISCUSSION

3.1 Temporal Evaluation of Indoor Atmospheric NCA Number Concentrations

Common household activities such as boiling water, cooking, burning scented candles, and mopping with a popular terpene-rich cleaning agent were found to produce a significant pool of indoor atmospheric NCA (Fig. 2). Emissions of NCA began immediately with the start of indoor activities, as evidenced by a steady increase in N_{NCA} [cm^{-3}], which is defined as the size-integrated NCA number concentrations from 1.18 to 3 nm, starting from the 10-minute source introduction period. For activities such as boiling water, cooking, and burning scented candles, NCA are primarily emitted directly from the combustion flame (Patra et al., 2024). In contrast, during indoor mopping, NCA are formed as secondary products. This occurs through the oxidation of gas-phase monoterpenes and monoterpenoids emitted from the mopping agent, which then interact with indoor O_3 to form oxygenated VOCs (OVOCs); some of these OVOCs nucleate to produce NCA (Rosales et al., 2022).

The measured indoor atmospheric NCA number concentrations varied in both their temporal profile and magnitude, depending on the type of indoor activity. The peak N_{NCA} were highest during secondary NCA nucleation associated

with indoor mopping activities (N_{NCA}~7.4 x 10^7 cm^{-3}), followed by boiling water (N_{NCA}~1.5 x 10^7 cm^{-3}), cooking (N_{NCA}~1.0 x 10^7 cm^{-3}), and burning scented candles (N_{NCA}~3.8x 10^5 cm^{-3}). This underscores the significance of secondary NCA nucleation in residential settings, which can exceed that of primary NCA sources. Boiling water and cooking activities were performed on a propane gas stove, whose combustion flame appears to emit significantly more NCA than those from candle flames. NCA were detected throughout the duration of these source activities. However, this was not the case for cooking activities. For the initial six minutes, a very large pool of NCA was emitted from the propane gas combustion, similar to the emissions observed during boiling water activities. However, after the six-minute mark, as the cooking activities involved butter-based cooking, the melting butter began to generate visible fumes. These fumes produced larger cooking-associated aerosol particles, which scavenged the NCA emitted from the flame, resulting in a sharp decline in N_{NCA} concentrations post six minutes during cooking activities (Fig. 2). A detailed discussion of the interaction between NCA and larger particles can be found in Section 3.2.

Compared to other NCA sources, indoor atmospheric NCA number concentrations during the common household activities studied here are significantly higher than N_{NCA} levels reported during outdoor new particle formation events (N_{NCA}~10^2 – 10^5 cm^{-3}) (Kontkanen et al., 2017) and in outdoor traffic-influenced areas (N_{NCA}~10^4 – 10^5 cm^{-3}) (Rönkkö et al., 2017). Moreover, N_{NCA} levels from common household activities are also higher than those emitted indoors during the use of 3D printers (N_{NCA}~10^2 – 10^5 cm^{-3}) (Poikkimäki et al., 2019) and from indoor NCA emissions resulting from the ozonolysis of skin oils (N_{NCA}~10^2 cm^{-3}) (Yang et al., 2021). Given the prevalence of these activities in homes and their typical occurrence in the presence of occupants, there is a potential for significant respiratory exposure to NCA during these activities (as discussed in Section 3.3).

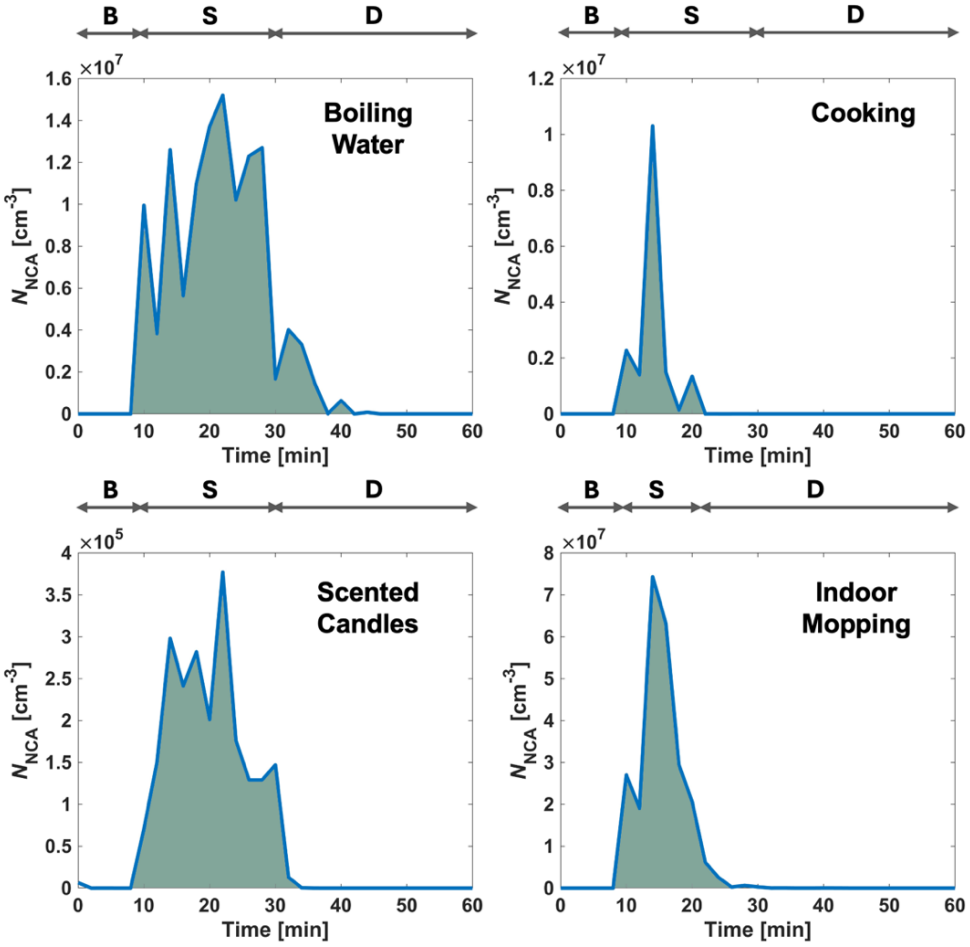

Figure 2: Temporal evaluation of indoor atmospheric NCA number concentrations during representative (top-left) boiling water, (top-right) cooking grilled cheese sandwiches, (bottom-left) scented candle combustion, and (bottom-right) indoor mopping activities (B: background period; S: source event period; D: decay period).

3.2 Indoor Atmospheric NCA Dynamics in Residential Buildings

Indoor atmospheric NCA formation and transformation during common household activities are highly transient, as evidenced by the rapid changes in NCA number concentrations (Fig. 2). These dynamics are influenced by a balance between NCA production and loss processes (equations 1 and 2), where production is continuously occurring during various activities, and loss is predominantly governed by coagulation with larger particles, as quantified for a representative activity in Table 1. To further illustrate this, we demonstrate the relationship between NCA apparent emission rates and net indoor coagulation sinks during activities such as boiling water and cooking indoors (Fig. 3). Apparent NCA emission rates are inversely related to the net coagulation potential of the indoor atmosphere (Fig. 3). As discussed in Section 3.1, a sharp decline in NCA number concentrations was observed during cooking activities, which coincided with the appearance of visible fumes from melting butter. These fumes significantly increased the coagulation potential of the indoor atmosphere, leading to a significant reduction in the apparent NCA emission rates. To quantify, our measurements indicate that NCA can persist in indoor air throughout the duration of common household activities or until rates of intermodal coagulation scavenging surpass those observed in heavily polluted urban atmospheres (where $CoagSnk_{Net}$ > 0.2 s^{-1}).

Additionally, we show that combustion-generated indoor NCA do not exhibit a strong correlation with traditional combustion markers, such as NO_x mixing ratios (Fig. 3) and $PM_{2.5}$ mass concentrations (with a Pearson correlation of ~-0.35). Therefore, our findings indicate that indoor atmospheric NCA cannot be accurately modeled simply by measuring traditional markers such as indoor NO_x and $PM_{2.5}$, which are insufficient for accurately predicting NCA number concentrations. This is due to the various physical processes and building-related factors that contribute to size-resolved indoor NCA dynamics (equations 1 and 2). Instead, indoor atmospheric NCA should be measured directly using high-resolution online nanoparticle instrumentation.

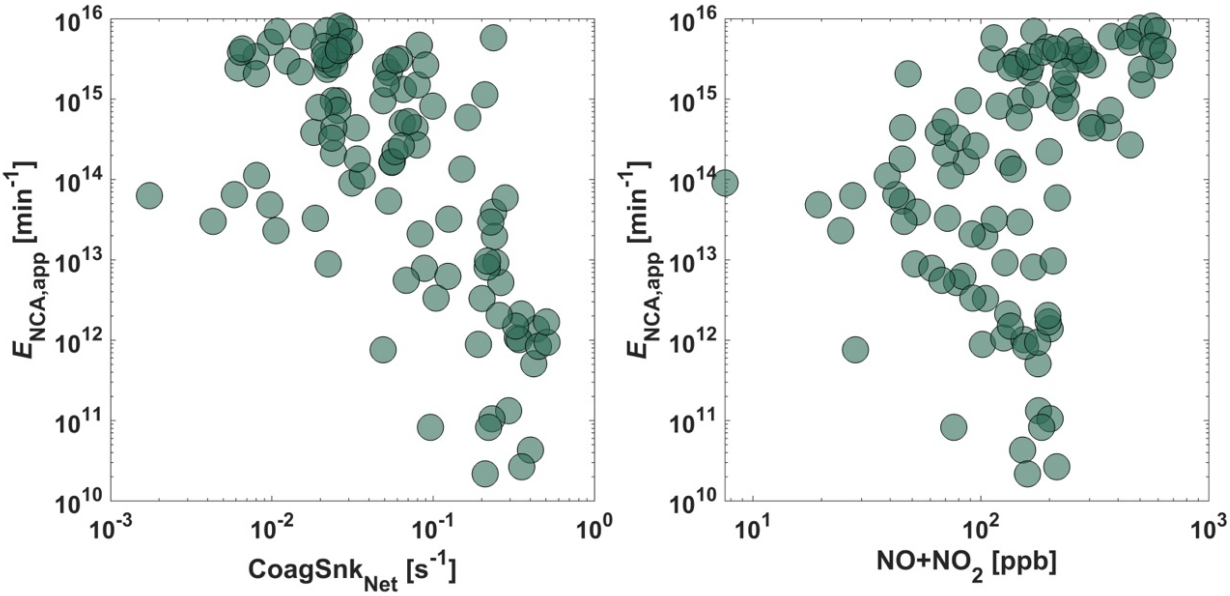

Figure 3: Relationship between indoor atmospheric NCA apparent emission rates and (left) net indoor coagulation sinks, and (right) NO_x mixing ratios during indoor boiling water and cooking activities.

Condensation is another process that significantly affects the transformation of indoor atmospheric NCA. We observed that the condensational growth of freshly emitted NCA to larger particles is remarkably high during common household activities. For example, butter-based indoor cooking was marked with mean condensational growth rates of 48 nm h^{-1} in the size range of 3–25 nm. Additionally, intramodal coagulation of smaller particles can also serve as a source of indoor atmospheric NCA, particularly from strong indoor NCA sources such as boiling water (coagulation as a source process can contribute up to 40% to the dynamics of indoor atmospheric NCA). Due to the very short coagulation lifetimes of NCA, coagulation losses dominate compared to ventilation and deposition losses in indoor environments. Therefore, given that the dynamics of indoor atmospheric NCA are sensitive to coagulation, it is crucial

to accurately account for both intermodal and intramodal coagulation of NCA to properly model the emission rates and condensational growth of indoor atmospheric NCA.

Table 1: Mean relative contribution of physical processes to the indoor atmospheric apparent NCA emission rates during indoor cooking activities in the Purdue zEDGE test house.

Physical Process	Relative Contribution ± Standard Error [%]
Coagulation Source	0.10 ± 0.052
Coagulation Sink	75.96 ± 1.867
Condensation Source	11.05 ± 1.474
Condensation Loss	11.10 ± 0.835
Deposition	0.09 ± 0.004
Ventilation	0.03 ± 0.003

3.3 Indoor Atmospheric NCA Inhalation Exposures in Residential Buildings

Due to the significant presence of indoor atmospheric NCA during common household activities, the human inhalation respiratory burden to indoor atmospheric NCA is also expected to be high. To investigate this, we determined the size-integrated NCA respiratory tract deposited dose rates ($R_{D,NCA}$; min^{-1}) for adults during these activities (Jiang et al., 2021). The size-integrated NCA respiratory tract deposited dose rates scaled with the apparent NCA emission rates (Fig. 4), suggesting a higher respiratory burden during strong indoor atmospheric NCA emission events. For instance, a 20-minute boiling water activity can deposit about 10^{12} NCA in the adult respiratory system. The largest portion of this dose is received in the head airways, followed by the tracheobronchial region, and finally the pulmonary region in humans. Given the high NCA respiratory tract deposited dose rates observed during common household activities, the potential health impacts are a significant concern. Activities such as boiling water, cooking, and cleaning, which are ubiquitous and frequently repeated throughout the day, can lead to substantial cumulative exposure to NCA for occupants. This underscores the urgent need for strategies to control indoor atmospheric NCA levels to protect occupant health, considering the frequent and prolonged exposure that is typical in residential settings.

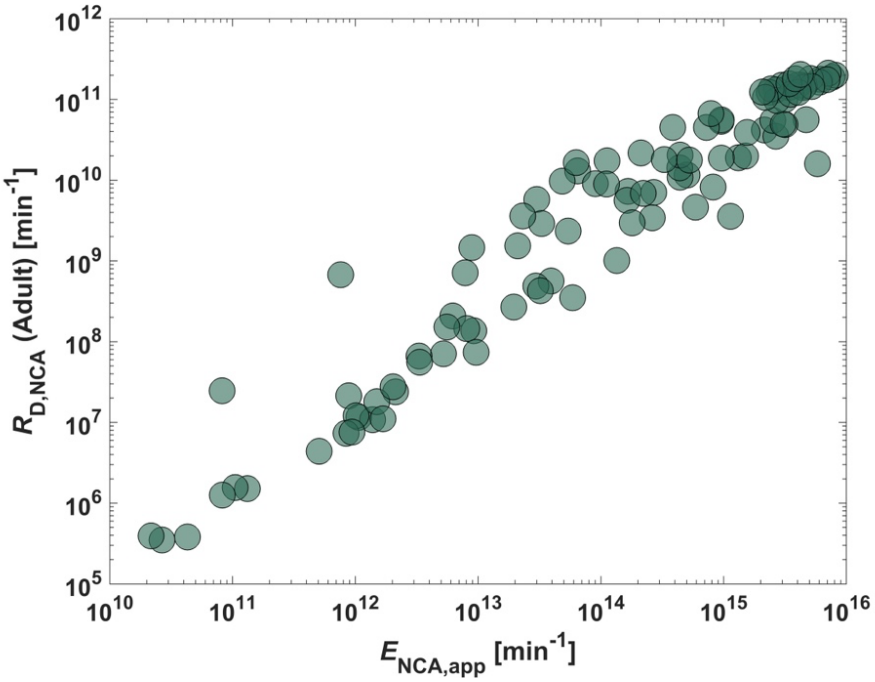

Figure 4: Relationship between indoor atmospheric NCA apparent emission rates and size-integrated NCA respiratory tract deposited dose rates for adults during indoor boiling water and cooking activities.

High performance buildings that are appropriately designed and operated can help manage indoor atmospheric NCA concentrations and exposures. As discussed in this study, our NCA general dynamics model demonstrates that indoor atmospheric NCA concentrations result from a balance between production and loss processes. Activities identified here act as significant sources of indoor atmospheric NCA, which directly influence the size-integrated NCA respiratory tract deposited dose. To counteract these effects, accelerating the loss processes is essential. Although inherent physical processes such as coagulation and condensation cannot be directly controlled, building-related factors are adjustable, and high performance building controls can significantly impact indoor atmospheric NCA levels. High performance buildings can employ designs that integrate NCA monitoring with ventilation controls. Whenever high NCA concentrations are detected, the controls allow additional exhaust systems to activate automatically, increasing the overall mechanical ventilation rate. For instance, kitchen exhaust hoods equipped with these controls can be particularly effective when gas stoves are in use. Additionally, the opening of windows can also be controlled using the same logic to further facilitate natural ventilation, thereby diluting indoor NCA concentrations. The strategic placement of filter-based air purifiers, which respond to real-time NCA data, can further enhance indoor air quality. All these strategies correspond to the loss processes outlined in equation 1 and can minimize indoor NCA concentrations. Thus, our findings support the integration of precise NCA measurements with innovative building design to substantially mitigate the respiratory burden of NCA in residential indoor environments.

4. CONCLUSIONS

This study offers critical insights into the dynamics and potential respiratory burden of indoor atmospheric nanocluster aerosol (NCA) in residential buildings, underscoring the importance of understanding NCA dynamics and transformations. Through comprehensive field measurements and modeling within a mechanically ventilated residential environment, we demonstrated that indoor activities such as boiling water, cooking, and indoor mopping can significantly elevate indoor atmospheric NCA concentrations, surpassing those associated with outdoor NCA sources. The primary mechanisms for NCA loss, coagulation followed by condensation, deposition, and ventilation, highlight the complex interplay of factors influencing indoor NCA dynamics. This complexity necessitates accurate modeling of these processes in studies of indoor NCA dynamics. Given the significant portion of time humans spend indoors, the heightened exposure to indoor atmospheric NCA, especially during common household activities, raises concerns for public health. Our findings stress the inadequacy of conventional indoor air quality markers to model NCA dynamics, calling for more field measurement campaigns to monitor indoor atmospheric NCA. Furthermore, our model suggests that high performance buildings can effectively manage indoor atmospheric NCA concentrations by integrating NCA monitoring with automated ventilation and air purifying systems. These strategic interventions can substantially mitigate the respiratory burden of NCA in residential environments.

NOMENCLATURE

$N_{d_{p,i}}$	Indoor particle number concentrations in size bin i as characterized by the midpoint diameter, d_p, in the PSMPS [# cm^{-3}]
$N_{out,d_{p,i}}$	Outdoor particle number concentrations in size bin i as characterized by the midpoint diameter, d_p, in the PSMPS [# cm^{-3}]
$dN_{d_{p,i}}/dt$	Time derivative of $N_{d_{p,i}}$ [cm^{-3} min^{-1}]
$E_{d_{p,i,app}}$	Size-dependent apparent emission rate of particles at size d_p [cm^{-3} min^{-1}]
$k_{vent,m}$	Nominal outdoor air ventilation rates through mechanical ventilation [min^{-1}]
$k_{vent,n}$	Nominal outdoor air ventilation rates through natural ventilation [min^{-1}]
$k_{vent,l}$	Nominal outdoor air ventilation rates through infiltration [min^{-1}]
$\eta_{d_{p,i}}$	Size-dependent single-pass removal efficiency of the filter used in the mechanical ventilation system [-]
$P_{d_{p,i}}$	Size-dependent penetration efficiency of particles across the leakage flow path [-]
$k_{ap,d_{p,i}}$	Size-dependent first-order removal rate coefficient of particles at size d_p through a filter-based air purifier [min^{-1}]
$k_{dep,d_{p,i}}$	Size-dependent first-order deposition loss rate coefficient of particles at size d_p [min^{-1}]

$CoagSnk_{d_{p,i}}$	Coagulation sink of particles at size d_p [min^{-1}]
$CoagSrc_{d_{p,i}}$	Coagulation source of particles at size d_p [cm^{-3} min^{-1}]
$Cond_{d_{p,i}}$	Net condensational loss of particles at size d_p due to the condensation of low volatility vapors [cm^{-3} min^{-1}]
$Cond_{(d_{p,i-1})}$	Net condensational source of particles at size d_p due to the condensation of low volatility vapors [cm^{-3} min^{-1}]
$CoagSnk_{Net}$	Net difference between the coagulation sink and the source [min^{-1}]
GR_{Cond}	Net condensational growth rate of particles [nm h^{-1}]
NCA	Sub-3 nm nanocluster aerosol
$R_{D,NCA}$	Size-integrated NCA respiratory tract deposited dose rates [min^{-1}]
N_{NCA}	Size-integrated NCA number concentrations [# cm^{-3}]

REFERENCES

Audignon-Durand, S., Ramalho, O., Mandin, C., Roudil, A., Le Bihan, O., Delva, F., & Lacourt, A. (2023). Indoor exposure to ultrafine particles related to domestic activities: A systematic review and meta-analysis. *Science of The Total Environment*, *904*, 166947. https://doi.org/https://doi.org/10.1016/j.scitotenv.2023.166947

Jiang, J., Ding, X., Patra, S. S., Cross, J. N., Huang, C., Kumar, V., Price, P., Reidy, E. K., Tasoglou, A., Huber, H., Stevens, P. S., Boor, B. E., & Jung, N. (2023). Siloxane Emissions and Exposures during the Use of Hair Care Products in Buildings. *Environmental Science & Technology*, *57*(48), 19999–20009. https://doi.org/10.1021/acs.est.3c05156

Jiang, J., Ding, X., Tasoglou, A., Huber, H., Shah, A. D., Jung, N., & Boor, B. E. (2021). Real-Time Measurements of Botanical Disinfectant Emissions, Transformations, and Multiphase Inhalation Exposures in Buildings. *Environmental Science & Technology Letters*, *8*(7), 558–566. https://doi.org/10.1021/acs.estlett.1c00390

Kangasluoma, J., Cai, R., Jiang, J., Deng, C., Stolzenburg, D., Ahonen, L. R., Chan, T., Fu, Y., Kim, C., Laurila, T. M., Zhou, Y., Dada, L., Sulo, J., Flagan, R. C., Kulmala, M., Petäjä, T., & Lehtipalo, K. (2020). Overview of measurements and current instrumentation for 1–10 nm aerosol particle number size distributions. *Journal of Aerosol Science*, *148*, 105584. https://doi.org/https://doi.org/10.1016/j.jaerosci.2020.105584

Kontkanen, J., Lehtipalo, K., Ahonen, L., Kangasluoma, J., Manninen, H. E., Hakala, J., Rose, C., Sellegri, K., Xiao, S., Wang, L., Qi, X., Nie, W., Ding, A., Yu, H., Lee, S., Kerminen, V.-M., Petäjä, T., & Kulmala, M. (2017). Measurements of sub-3nm particles using a particle size magnifier in different environments: from clean mountain top to polluted megacities. *Atmospheric Chemistry and Physics*, *17*(3), 2163–2187. https://doi.org/10.5194/acp-17-2163-2017

Kulmala, M., Petäjä, T., Nieminen, T., Sipilä, M., Manninen, H. E., Lehtipalo, K., Dal Maso, M., Aalto, P. P., Junninen, H., Paasonen, P., Riipinen, I., Lehtinen, K. E. J., Laaksonen, A., & Kerminen, V.-M. (2012). Measurement of the nucleation of atmospheric aerosol particles. *Nature Protocols*, *7*(9), 1651–1667. https://doi.org/10.1038/nprot.2012.091

Liu, J., Jiang, J., Ding, X., Patra, S. S., Cross, J. N., Huang, C., Kumar, V., Price, P., Reidy, E. K., Tasoglou, A., Huber, H., Stevens, P. S., Boor, B. E., & Jung, N. (2024). Real-time evaluation of terpene emissions and exposures during the use of scented wax products in residential buildings with PTR-TOF-MS. *Building and Environment*, *255*, 111314. https://doi.org/https://doi.org/10.1016/j.buildenv.2024.111314

Patra, S. S., Jiang, J., Ding, X., Huang, C., Reidy, E. K., Kumar, V., Price, P., Keech, C., Steiner, G., Stevens, P., Jung, N., & Boor, B. E. (2024). Dynamics of nanocluster aerosol in the indoor atmosphere during gas cooking. *PNAS Nexus*, *3*(2), pgae044. https://doi.org/10.1093/pnasnexus/pgae044

Peters, A., Rückerl, R., & Cyrys, J. (2011). Lessons from air pollution epidemiology for studies of engineered nanomaterials. *Journal of Occupational and Environmental Medicine*, S8–S13. https://doi.org/10.1097/JOM.0b013e31821ad5c0

Poikkimäki, M., Koljonen, V., Leskinen, N., Närhi, M., Kangasniemi, O., Kausiala, O., & Dal Maso, M. (2019). Nanocluster Aerosol Emissions of a 3D Printer. *Environmental Science & Technology*, *53*(23), 13618–13628. https://doi.org/10.1021/acs.est.9b05317

Rönkkö, T., Kuuluvainen, H., Karjalainen, P., Keskinen, J., Hillamo, R., Niemi, J. V, Pirjola, L., Timonen, H. J., Saarikoski, S., Saukko, E., Järvinen, A., Silvennoinen, H., Rostedt, A., Olin, M., Yli-Ojanperä, J., Nousiainen,

P., Kousa, A., & Dal Maso, M. (2017). Traffic is a major source of atmospheric nanocluster aerosol. *Proceedings of the National Academy of Sciences*, *114*(29), 7549–7554. https://doi.org/10.1073/pnas.1700830114

Rosales, C. M. F., Jiang, J., Lahib, A., Bottorff, B. P., Reidy, E. K., Kumar, V., Tasoglou, A., Huber, H., Dusanter, S., & Tomas, A. (2022). Chemistry and human exposure implications of secondary organic aerosol production from indoor terpene ozonolysis. *Science Advances*, *8*(8), eabj9156.

Sgro, L. A., Simonelli, A., Pascarella, L., Minutolo, P., Guarnieri, D., Sannolo, N., Netti, P., & D'Anna, A. (2009). Toxicological Properties of Nanoparticles of Organic Compounds (NOC) from Flames and Vehicle Exhausts. *Environmental Science & Technology*, *43*(7), 2608–2613. https://doi.org/10.1021/es8034768

Stolzenburg, D., Cai, R., Blichner, S. M., Kontkanen, J., Zhou, P., Makkonen, R., Kerminen, V.-M., Kulmala, M., Riipinen, I., & Kangasluoma, J. (2023). Atmospheric nanoparticle growth. *Reviews of Modern Physics*, *95*(4), 45002. https://doi.org/10.1103/RevModPhys.95.045002

Yang, S., Licina, D., Weschler, C. J., Wang, N., Zannoni, N., Li, M., Vanhanen, J., Langer, S., Wargocki, P., Williams, J., & Bekö, G. (2021). Ozone Initiates Human-Derived Emission of Nanocluster Aerosols. *Environmental Science & Technology*, *55*(21), 14536–14545. https://doi.org/10.1021/acs.est.1c03379

ACKNOWLEDGEMENTS

Financial support was provided by the National Science Foundation (CBET-1847493 to B.E.B.), the Alfred P. Sloan Foundation Chemistry of the Indoor Environments Program (G-2018-11061 to B.E.B.), and Purdue University start-up funds (to N.J.). The authors thank Jinglin Jiang, Xiaosu Ding, Chunxu Huang, Emily K. Reidy, Vinay Kumar, Paige Price, Connor Keech, and Philip S. Stevens for their assistance during the field measurement campaign.